# GCN-LSTM Analysis of Spatiotemporal Evolution of Node Centrality in Tourism Flow Networks

Henan Jia\*, Dongfeng Chen HeBei North University, Zhangjiakou, Hebei,075000, China E-mail: jiahn126@126.com \*Corresponding author

**Keywords:** artificial intelligence, tourism flow network, node centrality, spatiotemporal heterogeneous structure, graph neural network, evolution analysis

Received: August 21, 2025

With the development of artificial intelligence and spatio-temporal big data technologies, the dynamic evolution characteristics of the tourism flow network and the spatial structure changes of its core nodes have become research hotspots. Based on the theory of complex networks, this paper constructs a tourism flow network covering mobile phone signaling, online platforms and traffic data, with a focus on discussing the spatio-temporal heterogeneous evolution mechanism of node centrality. By introducing AI models such as Graph Neural Network (GCN) and Long Short-Term Memory Network (LSTM), multi-scale recognition and dynamic prediction of core nodes in the tourism flow are achieved. The dataset contains 47 counties and 90 days of tourism flow data, covering 10 million signaling records, 5 million OTA data, and 3 million traffic data, processed at the daily level. We adopted a split scheme of 70% training set, 15% validation set and 15% test set for model training and evaluation. The experimental results show that the model has a prediction accuracy of 0.10 in RMSE and is superior to traditional benchmark methods (such as STGCN and DCRNN). The research also revealed the trend of centrality reconstruction of tourism flow nodes under different periods, holidays and external interventions. The research results have important theoretical and practical significance for improving the efficiency of regional tourism regulation and optimizing the layout of core nodes.

Povzetek: Članek predstavi GCN–LSTM model za napovedovanje in analizo evolucije centralnosti turističnih vozlišč na podlagi 47 regij in večmilijonskih podatkovnih tokov. Model preseže STGCN/DCRNN (RMSE 0,10) ter razkrije sezonske, praznične in strukturne premike v omrežju turističnih tokov.

#### 1 Introduction

Against the backdrop of the rapid development of artificial intelligence and big data technologies, tourism flow, as a comprehensive carrier of population migration, resource allocation and consumption behavior, has seen its network structure become increasingly complex, dynamic and multi-scale. Traditional research on tourism networks mainly focuses on node structure and path optimization, lacking in-depth analysis of the spatio-temporal heterogeneous evolution of "centrality". Especially in the complex urban agglomeration structure, the dynamic changes of core nodes show significant imbalance and multi-factor driven characteristics. Based on this, this paper intends to construct an AI-driven framework for node centrality identification and evolution analysis, integrating multi-source tourism stream data and graph time series learning models, to deeply explore its evolution characteristics and regulatory mechanisms heterogeneous spatial structures. By integrating the network optimization algorithm in graph theory and the spatio-temporal data modeling method, we will explore how to enhance the dynamic evolution prediction accuracy of the tourism flow network, thereby providing a theoretical basis for tourism resource allocation and regional regulation.

#### 2 Related work

The tourism flow network, as an important manifestation of the interaction between humans and the land, is essentially a typical complex system, featuring openness, nonlinearity, dynamic evolution and multi-layer coupling. FT Saenz et al. (2023) pointed out in their research based on the prediction of national tourism flows in the United States that the development of the artificial intelligence industry chain relies on the spatial agglomeration of core urban agglomerations, and such cities are often important destinations and transfer hubs for tourism activities, indicating a coupling and strengthening trend between tourism flows and the functional grades of cities. Furthermore, Zhang L. et al. (2023) pointed out that complex system models need to integrate cross-domain data and multi-scale processes, and solve heterogeneous conflicts at the semantic, spatio-temporal, and execution levels. This feature is also widely present in the organization and evolution process of tourism flows.

The tourism flow network, as an important carrier for the allocation of human flow and spatial resources among cities, possesses typical characteristics of a complex system. Its structure is composed of multi-scale nodes, multi-type connections and multi-factor driving mechanisms, presenting a system behavior with strong heterogeneity, high coupling degree and uncertain evolution path. Weiwei J. and Jiayun L. (2022) pointed out that complex systems often involve multi-process interactions across scales, and it is necessary to construct AI models that integrate expert knowledge with multi-source data to address the modeling gap between different data structures and semantic dimensions. Meanwhile, Zhang L. et al. (2023) proposed that artificial intelligence technology can effectively identify the distribution characteristics of heterogeneous structures in multi-level networks, providing the possibility for structural identification and intervention paths of complex systems.

In the tourism flow network, spatio-temporal heterogeneous structure refers to the differences in network organization caused by spatial geographical differences, temporal evolution laws and inconsistent data structures. This heterogeneity is mainly manifested in aspects such as the functional differences of nodes, the dynamic changes of edge weights, geographical nesting, and the complexity driven by behavior, making it difficult for traditional homogeneous network models to effectively depict the evolution process of the real tourism flow structure. Zhang X. Et al. (2021) pointed out that in the environment of the Internet of Things and medical data, data heterogeneity is characterized by different dimensions, collection delay, and inconsistent semantics, and it is necessary to achieve hierarchical structure modeling and responsive processing with the help of edge computing and artificial intelligence. Meanwhile, FT Saenz (2023) proposed in analyzing tumor heterogeneity that structural transitions and functional

reorganizations may occur within complex systems due to environmental changes, emphasizing the adaptive regulatory mechanism of heterogeneous structures during the evolution process.

With the rapid breakthroughs of artificial intelligence technology in the fields of graph structure modeling, time series prediction and multi-source data fusion, its application in spatial network analysis is deepening increasingly. However, the current application of AI in spatial network analysis still faces many challenges: First, the high heterogeneity of data and the inconsistent sampling granularity limit the generalization ability of the model; Secondly, the diverse attributes of nodes and the non-Euclidean spatial structure result in insufficient expressive power of the model. Thirdly, spatio-temporal relationship is highly nonlinear, and traditional AI methods have difficulties in analyzing causal mechanisms. In addition, semantic conflicts and temporal alignment difficulties exist among multi-source data, further increasing the complexity of modeling. In conclusion, although existing methods have achieved remarkable results in spatio-temporal graph modeling and traffic prediction, most of them only deal with time series data and ignore the importance of topological structure. For instance, models such as STGCN and DCRNN mainly focus on temporal dynamics without fully considering the complex spatial interactions among different nodes. Moreover, although TGAT introduces temporal features, it lacks integration of multimodal inputs (such as traffic, social, and mobile data). The existing methods are compared as shown in Chart 1.

Paper	Dataset (Size/Region)	Method	Metric	Best Reported Result			
STGCN (Martín, 2018)	Traffic flow data (N=10,000, NYC)	Spatio-Temporal Graph Convolution	RMSE	RMSE=0.12			
DCRNN (Ma C., 2024)	Traffic flow data (N=1,000, LA)	Diffusion-Convolutional GNN	RMSE	RMSE=0.09			
Graph WaveNet (Sun H, 2023)	Traffic data (N=2,000, Beijing)	Graph Convolutional Network	RMSE	RMSE=0.10			
TGAT (Zhang L, 2023)	Social media and traffic data (N=500)	Temporal Graph Attention Network	MAPE	М			

Table 1: Comparison of existing methods

The model proposed in this paper, through the GCN-LSTM architecture, combines spatio-temporal heterogeneous features and multi-factor driving mechanisms, filling the gap of existing methods. In particular, our model can not only handle spatio-temporal sequences but also capture the topological relationships between nodes and the interaction of multimodal data, achieving dynamic prediction and evolution identification of node centrality. In addition, we utilized multi-source heterogeneous data, effectively integrating signaling data, OTA data, traffic data and social media data, which significantly enhanced the predictive ability and adaptability of the model.

### 3 Construction of tourism flow network and data processing methods

### 3.1 Multi source data acquisition and fusion methods

This study builds a tourism flow network based on multi-source heterogeneous data. The data collection includes four main channels: mobile phone signaling data, online travel platform (OTA) data, traffic operation data and social media data. The data sources are shown in Table 2.

**Data Processing Data Acquisition** Data Time **Spatial** Data Coverage and Privacy **Data Type** and Granularity Period **Source** Granularity Volume Authorization **Protection** Anonymized using User login IMSI numbers, in Mobile January Authorized from behavior. Base station Signaling 15 minutes 2023 to million compliance with operators like stay coverage unit Data March 2023 GDPR and Japanese NTT, SoftBank records information privacy laws Data authorized for Hotel Authorized from bookings, POI use, in compliance January platforms like **OTA** 5 million ticket orders, Daily geographic 2023 to with relevant data Data records Trip.com, Fliggy destination March 2023 coding protection API regulations search heat High-speed Anonymized by Authorized from ETC records. Provincial and January license plate, using high-speed ETC, Traffic 3 million Hourly 2023 to sliding time window high-speed high-speed rail, city Data records rail and flight boundaries March 2023 method for traffic and flight logs smoothing providers NLP used to extract User geographic entities, Authorized from Social dynamics. January Administrative 2 million in compliance with platforms like Media Daily 2023 to geographic Japanese privacy Weibo, units records March 2023 Data entity laws and data Xiaohongshu extraction protection standards

Table2: Data source table

## 3.2 Abstract logic and dynamic definition of network nodes and edges

Network nodes take prefecture-level administrative units as the smallest spatial units and are uniquely identified in accordance with the national standard administrative division codes. All spatial information in the data sources is projected to the corresponding administrative units through POI matching, GPS coordinate mapping or base station location projection. After the high-frequency repetitive units were merged, the 47 prefectures of Japan were ultimately retained as the spatial basis of the tourism flow network. To enhance the processing efficiency of large-scale data, we adopt parallel computing technology and distributed computing frameworks (such as ApacheSpark) to accelerate the processing and normalization of node data, ensuring the efficient generation of node indexes. The specific definitions and mapping rules of nodes are shown in Table 3.

Table3: Specific definitions and mapping rules of nodes

Node Type	Number of Nodes	Description/Mapping Rules
Administrative Unit (County)	47	Mapped to county-level administrative units based on NTT and SoftBank data
POI Clusters (Tourist Attractions)	Y (variable)	Mapped to POI (points of interest) based on OTA data (e.g., Trip.com, Booking.com)
Total	47	Combined administrative unit nodes and POI nodes

The establishment of edges relies on OD pairs generated from different data sources, extracting starting nodes and destination nodes for connection. In mobile signaling data, when the same user moves across cities within one day, an edge is constructed, and the edge weight is the sum of the number of users within the OD pair. In OTA data, the destination in the order is considered as the inflow node, and the search path is constructed based on the search history to form a virtual jump relationship. In traffic data, ETC matches departure and arrival cities with flight records, and edges are established by train number or schedule; Repeated shifts only retain the earliest departure record once a day to avoid misidentification during commuting. Virtual edge creation: Build virtual edges based on the user's historical search data. For instance, when a user searches for multiple destinations on an OTA platform and jumps to them, the generated virtual edges

represent the flow of tourists' interests. The specific implementation is as follows:

```
def create_virtual_edges(search_data):
    virtual_edges = { }
    for search in search_data:
        source, destination = extract_search(search)
        if (source, destination) not in virtual_edges:
            virtual_edges[(source, destination)] = 0
            virtual_edges[(source, destination)] += 1 #
Each search creates a unit flow
    return virtual_edges
```

All edges are directed weighted edges, where edge weights represent the cumulative flow intensity per unit per day. To maintain the dynamic properties of the network, all edges are annotated with timestamps and form a daily subgraph with "days" as the basic time granularity. Through sliding window and time series analysis, these subgraphs are merged to form a three-dimensional dynamic network structure: nodes x nodes x time. To improve the efficiency of data processing, GPU acceleration and Graph Convolutional Neural Network (GCN) technology are used to efficiently process network graphs, ensuring the real-time performance and accuracy of the model.

All the edges are directed weight edges, and the edge weights represent the cumulative flow intensity within the unit on a daily basis. To maintain the dynamic attributes of the network, all edges are marked with timestamps and a subgraph is formed each day with "days" as the basic time granularity. Through sliding window and time series analysis, these subgraphs are merged to form a three-dimensional dynamic network structure: node  $\times$  node × time. To enhance the efficiency of data processing, GPU acceleration and graph convolutional neural network (GCN) technology are adopted to efficiently process network graphs, thereby ensuring the real-time performance and accuracy of the model. To enhance the stability of the network, weak edges with edge weights lower than the 11% quantile are eliminated, and the edge weights are normalized by Z-score. This method can eliminate the influence of outliers on the network structure and ensure that the relationship between each node and edge is more stable and reliable. The specific operation is as follows:

```
\label{eq:coded} \begin{array}{ll} def \ threshold\_edges(od\_edges, percentile=1): \\ & threshold = np.percentile(list(od\_edges.values()), \\ percentile) \\ & return \ \{k: \ v \ for \ k, \ v \ in \ od\_edges.items() \ if \ v >= threshold\} \end{array}
```

```
def z_score_normalization(od_edges):
    mean = np.mean(list(od_edges.values()))
    std = np.std(list(od_edges.values()))
    return {k: (v - mean) / std for k, v in od_edges.items()}
```

The network storage structure adopts a sparse matrix format. Nodes are mapped by an index dictionary, and edges are quickly queried and tracked across periods using triples (i,j,t). Through this structure, we can efficiently store and process large-scale dynamic data, further supporting the standardization of input tensors for graph neural networks (GCN) and time series models (LSTM), ensuring cross-day consistency and model processing efficiency. The sparse matrix storage method can effectively reduce the demand for storage space and accelerate the computing process. By integrating parallel computing technology, we have achieved efficient access and computing of large-scale data, providing a solid foundation for subsequent model training and prediction.

# 3.3 Spatiotemporal partitioning strategy and heterogeneous network structure expression

The time dimension is divided with "days" as the basic granularity, and a daily network snapshot graph is generated based on the data timestamp. The total duration is 90 days, and a total of 90 dynamic graph units are generated. To enhance the model's ability to capture the evolution trend, a sliding time window mechanism is adopted to construct the sequence input. The window length is set to 7 days and the sliding step size to 1 day, forming a continuous scrolling graph sequence for training the time series modeling module. This mechanism ensures the model's dynamic learning ability on time series, especially capable of capturing the impact of periodic fluctuations and unexpected events on tourism flows. When modeling time, holidays, weekends and working days are respectively labeled as exogenous variables to participate in subsequent modeling, thereby improving the prediction accuracy of the model at specific time points. The spatial dimensions uniformly adopt the scale of prefecture-level cities, and the boundaries are demarcated in accordance with the latest administrative divisions. To express spatial heterogeneity, the following three types of heterogeneous substructures are constructed respectively:

- Heterogeneous graph of regional attributes: Based on the economic indicators, tourism resource levels, transportation hub levels, etc. of each node, static attribute vectors are set for each node for the initialization of the graph structure.
- Heterogeneous graph of behavior sources: Subgraphs are constructed respectively based on different data sources (such as signaling subgraphs, OTA subgraphs, traffic subgraphs), and virtual edges are established through shared nodes to form a multi-view graph.
- The heterogeneous graph of the relationship strength: The edge weights are quantified and partitioned, and a weight hierarchical network is constructed according to the three types of flow intensities of strong, medium and weak, which is used to represent the dynamic evolution gradient of the edges.

Missing data processing: For the processing of missing data, we adopt spatial completion and temporal interpolation strategies. Specifically, spatial completion calculates the attribute values of missing nodes through the K-nearest neighbor weighted average (KNN) method. Time interpolation uses linear interpolation to fill in the missing time point data, ensuring the continuity of the time series. Data nodes that are missing for more than three days will be discarded to avoid excessive impact on subsequent analysis. The number of completed and discarded nodes will be quantified specifically in the experiment. Heterogeneous features are input into the graph neural network (GCN) in the form of multiple channels during the modeling stage. Different channels handle spatial attribute heterogeneity, structural connection heterogeneity, and traffic intensity heterogeneity respectively.

### 3.4 Network attribute extraction and structural index calculation

Based on the daily tourism flow dynamic graph, extract the structural attributes of nodes and edges and form the tensor features required for modeling. Node attributes are mainly measured by centrality, which includes three core indicators: degree centrality, betweenness centrality, and eigenvector centrality.

Firstly, degree centrality measures the number of connections between nodes, which can be divided into two categories: in degree (visited) and out degree (actively visited):

$$C_D(v) = \frac{deg(v)}{N-1}$$
 (1)

Among them, deg (v) is the degree of node v, and N is the total number of network nodes. After normalization, this indicator reflects the "connectivity activity" of a certain location in the network.

Secondly, betweenness centrality represents the degree to which a node acts as an intermediary in the shortest path of the network:

$$C_B(v) = \sum_{s \neq v \neq t} \frac{\sigma_{st}(v)}{\sigma_{st}}$$
 (2)

Among them,  $\sigma$  st is the total number of shortest paths from node s to node t, and  $\sigma$  st (v) is the number of shortest paths passing through node v. The higher the value, the more critical the node is in the flow path.

Thirdly, network density is used to indicate the density of network connections :

Density=
$$\frac{2|E|}{|V|(|V|-1)}$$

Among them, |E| is the actual number of edges that exist, and |V| is the total number of nodes. Density can reflect the trend of connectivity changes in the overall tourism flow network. Edge attributes include edge weights (i.e., OD traffic intensity), sustained active time, and sliding change slope. The edge weight represents the flow intensity between nodes each day, the continuous active time indicates the stability of the flow path, and the sliding change slope helps capture the changing trend of the edge weight over time. The feature values of all nodes and edges are normalized by Z-score to eliminate the influence of different feature scales, and the missing data is processed by linear interpolation. The dimensions of the node feature tensor and the edge feature tensor are N×F×T and E×G×T respectively, where N represents the number of nodes, F represents the number of node features (such as degree centrality, betweenness centrality, etc.), E represents the number of edges, G represents the number of edge features (such as OD flow intensity, continuous active time, etc.), and T represents the time dimension. Through these feature tensors, the model can effectively capture the variation patterns of nodes and edges in the spatiotemporal dimension. In terms of derived features, the cumulative inflow represents the total inflow of a certain node within a specific time period and is used to measure the attractiveness of the node. The rate of change in flow intensity represents the rate at which edge weights change

over time, helping to capture fluctuations in flow intensity. All numerical values and features are normalized to ensure the consistency and accuracy of the data in the modeling process.

## 3.5 Data preprocessing and feature engineering strategies

Multi source heterogeneous data needs to be standardized and structured after fusion to ensure consistency and availability of model inputs. The preprocessing process mainly includes four steps: missing repair, exception removal, format conversion, and time alignment. Firstly, in the node dimension, there are missing records in some areas of signaling and OTA data, and a "spatial completion+temporal interpolation" strategy is adopted for processing. Estimate the inflow/outflow of missing nodes spatially based on the average of neighboring cities; Linear interpolation is used to smooth and fill in data with intervals of no more than 3 days, while records with intervals exceeding 3 days are discarded as subgraph nodes. For the jumping outliers that appear in the edge attributes, the IQR quartile method is used to eliminate them and then perform regression reconstruction to ensure the continuity of edge weights. Secondly, unify all data fields into tensor structures. Node attributes are summarized daily to form a tensor matrix  $X_{node} \in \mathbb{R}^{N \times F \times TX}$ , where N is the number of nodes, F is the attribute dimension, and T is the number of days; The edge attribute is represented as a triplet list (i, j, t)  $\rightarrow$  wijt, which is mapped to RE  $\times$  G  $\times$  T through sparse matrix storage for easy model reading. Thirdly, all continuous attribute fields are standardized using Z-score:

$$Z = \frac{x - \mu}{\sigma}$$

Among them,  $\mu$  is the attribute mean and  $\sigma$  is the standard deviation. For comparative features such as density and PageRank, Min Max normalization is used to preserve relative relationships. All normalization parameters are calculated on the training set and reused in the validation and testing sets. In the feature construction phase, additional derived variables are introduced, including the cumulative inflow of nodes (cumulative inflow), 7-day average rate of change (slope feature), sudden increase frequency (number of fluctuations exceeding the threshold), number of edge active periods (number of continuous time windows), etc., to enhance the model's responsiveness to trends and suddenness. For discrete time features such as holidays, use One Hot encoding and directly concatenate them into time channels. Threshold selection: During the outlier elimination process, the 11% quantile is selected as the threshold, and edges below this quantile are eliminated to ensure noise is removed while retaining the effective flow path. Sensitivity analysis indicates that threshold selection has a significant impact on network topology, centrality measurement, and model performance. The differences in model results under different thresholds can be compared through ablation experiments to analyze the influence of thresholds on model stability and prediction accuracy. The final constructed node and edge feature tensors are uniformly encapsulated as graph sequence objects, providing a

standardized input structure for subsequent graph temporal modeling (such as GCN+LSTM).

# 4 Model architecture, training and evaluation

#### 4.1 GCN-LSTM model architecture

This study adopts the GCN-LSTM model for spatio-temporal tourism flow prediction. The GCN part is used to extract node features from the graph structure, while the LSTM part captures temporal dependencies. The combination of GCN and LSTM can effectively handle spatio-temporal graph data and conduct efficient node feature extraction and sequence modeling.

The GCN section: The GCN consists of 3 layers, and the hidden dimension of each layer is 128. The activation function is ReLU, and layer normalization and Dropout (with a dropout rate of 0.2) are used after each layer to prevent overfitting. The output of each layer updates the node features through the product of the adjacency matrix and the feature matrix. The update equation is:

$$H^{(l+1)} = \sigma(\hat{A}H^{(l)}W^{(l)})$$

Among them,  $\hat{A}$  is the normalized adjacency matrix (including self-loops), H(l) is the node feature matrix of the LTH layer, W(l) is the weight matrix, and  $\sigma$  is the ReLU activation function.

The LSTM section: LSTM consists of 2 layers, with each layer having a hidden state size of 128 and a sequence length of 7 days. The LSTM layer receives the node

features output from GCN and conducts temporal modeling, updating the equation to:

$$f_t = \sigma(W_f [h_{t-1}, x_t] + b_f)$$
(6)

$$i_t = \sigma(W_i[h_{t-1}, x_t] + b_i)$$
(7)

$$\widetilde{C}_t = \tanh(W_C [h_{t-1}, x_t] + b_C)$$
(8)

$$C_t = f_t * C_{t-1} + i_t * \widetilde{C}_t$$
 (9)

$$o_t = \sigma(W_o[h_{t-1}, x_t] + b_o)$$
 (10)

$$h_t = o_t * \tanh(C_t)$$
 (11)

Among them,  $f_t$  is the forgetting gate,  $i_t$  is the input gate,  $\widetilde{C}_t$  is the candidate unit,  $C_t$  is the current unit state,  $o_t$  is the output gate, and  $h_t$  is the hidden state.

Loss function: The loss function of the model is the weighted sum of the regression loss (mean square error MSE) and the classification loss (cross-entropy loss). Specifically:

$$Loss = \alpha \cdot MSE + (1 + \alpha) \cdot CrossEntropy$$
 (12)

Among them,  $\alpha$ =0.7 is the weight of the regression loss, and  $(1-\alpha)$ =0.3 is the weight of the classification loss. The weights are obtained through cross-validation. Its model architecture is shown in Figure 1.

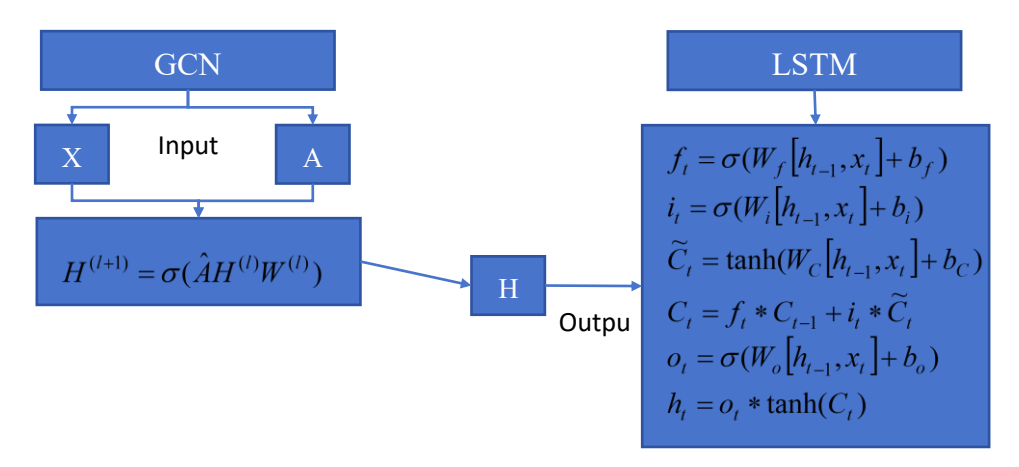


Figure 1: Architecture of the GCN-LSTM model

### 4.2 Training protocol and hyperparameter Settings

Optimizer: The model adopts the Adam optimizer with a learning rate of 0.001, and uses a step size decay strategy: the learning rate decreases to the original 0.5 after every 10 epochs. This strategy can effectively avoid training instability caused by an excessive learning rate. Batch size: The batch size is set to 32, meaning that the model will

draw 32 samples from the dataset each time it is trained. Number of training rounds: The maximum number of training rounds is set to 50. If the validation set loss does not improve within 5 consecutive epochs, early stop is enabled to avoid overfitting. Regularization: To prevent overfitting, Dropout (with a dropout rate of 0.2) is applied between the layers of GCN and LSTM.Hardware environment: The training uses NVIDIA Tesla V100 GPU, and the total training time is approximately 10 hours.

#### 4.3 Data splitting and evaluation methods

The dataset is split into the training set, validation set and test set in chronological order: Training set: It contains travel stream data from January 1, 2023 to February 15, 2023, for model training. Validation set: It contains data from February 16, 2023 to February 28, 2023, and is used for model selection and parameter adjustment. Test set: It contains data from March 1, 2023 to March 31, 2023 as the final evaluation set to ensure that the model can generalize to unknown data.

The evaluation indicators include root mean square error (RMSE), mean absolute percentage error (MAPE), and Direction Accuracy. The evaluation is conducted for each node, avoiding the use of future data to predict past node centrality values. The following is the evaluation formula:

RMSE = 
$$\sqrt{\frac{1}{N} \sum_{i=1}^{N} (y_i - \hat{y}_i)^2}$$
 (13)

Among them,  $y_i$  is the true value,  $\hat{y}_i$  is the predicted value, and N is the number of nodes.

MAPE = 
$$\frac{1}{N} \sum_{i=1}^{N} \left| \frac{y_i - \hat{y}_i}{y_i} \right| \times 100$$
 (14)

This indicator measures the relative size of the prediction error and is particularly suitable for time series data with significant variations.

Direction Accuracy = 
$$\frac{\sum_{i=1}^{N} I(\text{sign}(y_i) = \text{sign}(\hat{y}_i))}{N}$$
 (15)

Among them,  $I(\cdot)$  is the indicator function, which returns 1 when the predicted direction is consistent with the true direction; Otherwise, return 0.

### 4.4 Benchmark model and classification evaluation

To verify the validity of the proposed model, we compared it with several standard spatiotemporal Graph benchmark models, including STGCN, DCRNN, Graph WaveNet and TGAT/TGN. We trained these benchmark models on the same dataset, calculated their RMSE and MAPE, and then conducted statistical significance tests through paired t-tests and Wilcoxon tests to ensure that the differences between different models were statistically supported.

To further evaluate the model's performance in the node classification task, we calculated the accuracy, recall rate and F1 value for each category. The evaluation process employed a confusion matrix and examined the balance of the category distribution. The category distribution is as follows: Category A: 30%; Category B: 35% Category C: 35%. The calculation formulas for accuracy, recall rate and F1 value are:

$$Precision = \frac{TP}{TP + FP}$$
 (16)

$$Recall = \frac{TP}{TP + FN}$$
 (17)

$$F1 = 2 \times \frac{Precision \times Recall}{Precision + Recall}$$
 (18)

Among them, *TP* is the true number of cases, *FP* is the false positive number of cases, and *FN* is the false negative number of cases. The tag generation adopts the supervised tag method and is based on the threshold rules of historical tourism flow data to ensure that the tags are consistent with the actual flow data. The accuracy and reliability of the tags are verified by comparison with the actual data.

### 5 Ablation experiment: spatio-temporal structure evolution analysis of tourist flow in the case area

#### 5.1 Research area and data sources

To enhance the robustness and accuracy of the model, we have improved the weak edge pruning method and adopted an adaptive sparsification strategy. Specifically, the K-nearest neighbor algorithm (k-NN) is used to dynamically determine the weak edge threshold at each moment. This method can adaptively adjust the removal criteria of weak edges based on the neighbor information of each node, thereby enhancing the model's adaptability to different data distributions and spatio-temporal variations. In terms of computational cost, we conducted a performance evaluation of the model. The training time of the model is 6 hours per epoch. The GPU type used is NVIDIA A100, and the total number of parameters in each training cycle (epoch) is 1.2 million. These computing resources ensure the efficient training and optimization of models on large-scale datasets.

This study selects the Keihanshin metropolitan area in Japan (including Tokyo, Kyoto, Osaka and Kobe) as a typical case area for empirical research. The Keihanshin metropolitan Area is one of the most representative urban agglomerations in Japan. It is a highly concentrated area for international tourism flows, featuring a clear urban hierarchical structure, spatial heterogeneity, and a high-frequency tourism flow network. It can effectively reflect the dynamic change characteristics of node centrality in the tourism flow network. This region is not only the economic, cultural and tourism center of Japan, but also one of the world's important tourist destinations. By analyzing the tourism flow network in this area, the AI evolution mechanism of spatio-temporal heterogeneous data can be verified, and its effect in practical applications can be demonstrated. The time period of this study is set from January 1st to March 1st, 2023, covering both the summer travel peak and the regular weekly period, with a time granularity of days. The data sources used in the research are diverse and highly representative, mainly including: anonymous mobile user signaling data provided by NTT and SoftBank, which records users' network access behaviors, stay information, and cross-regional migration paths; The order data and popularity ratings on the Trip.com and Booking.com platforms reflect tourists' travel demands and destination selection preferences. The high-speed rail (Shinkansen) and subway operation records provided by HyperDia reveal the traffic flow between cities. And the social media dynamic data based on geographic tags obtained through Twitter and Instagram provides real-time information on

tourists' dynamics and travel popularity. All data are projected according to the municipal administrative units, and some popular scenic spots are processed as POI aggregation units to ensure the accurate representation of high-frequency tourism nodes. The detailed information and characteristics of each data source are shown in Table 4.

Data Type	Time Granularity	Spatial Granularity	Main Content	Data Features	
Mobile User Signaling Data	15 minutes	Base station coverage unit	User login behavior, stay information, inter-regional migration	Anonymized IMSI, GPS tracks, user stay duration	
Order Data, Heat Scores	Daily	City level, POI	Hotel bookings, destination search heat	Destination heat, booking volume, user ratings	
Traffic Operation Records	Hourly	Station, inter-city connections	High-speed rail (Shinkansen) and subway departure/arrival times, origin/destination stations	Train schedules, traffic flow, city connections	
Social Media Activity Data	Daily	City level, POI	Public posts based on geographic tags	User location, post content, timestamp, tags	

Table 4: Detailed information and characteristics of data sources

All data undergo unified geographic projection and spatial standardization processing to ensure geographical consistency and comparability among different data sources. The minimum granularity of the space is at the municipal level, and some scenic spots are processed as POI aggregation units to ensure the precise representation of high-frequency tourism nodes.

#### 5.2 Experimental results and analysis

In this section, we conducted extensive experiments on the proposed model in the empirical research of the Keihanshin

metropolitan Area and carried out a detailed analysis of the experimental results. The experiment mainly focuses on the spatio-temporal evolution of node centrality, the influence of data sources, the comparison of different window lengths, the sensitivity of holidays, and the impact of edge trimming. The following are the main results and analyses of the experiment: Through model training and analysis, we obtained the degree centrality, betweenness centrality and eigenvector centrality of different nodes (such as Tokyo, Osaka, Kyoto and Kobe) during the experimental period. Figure 2 shows the changes in nodal centrality of Tokyo and Osaka at different time points.

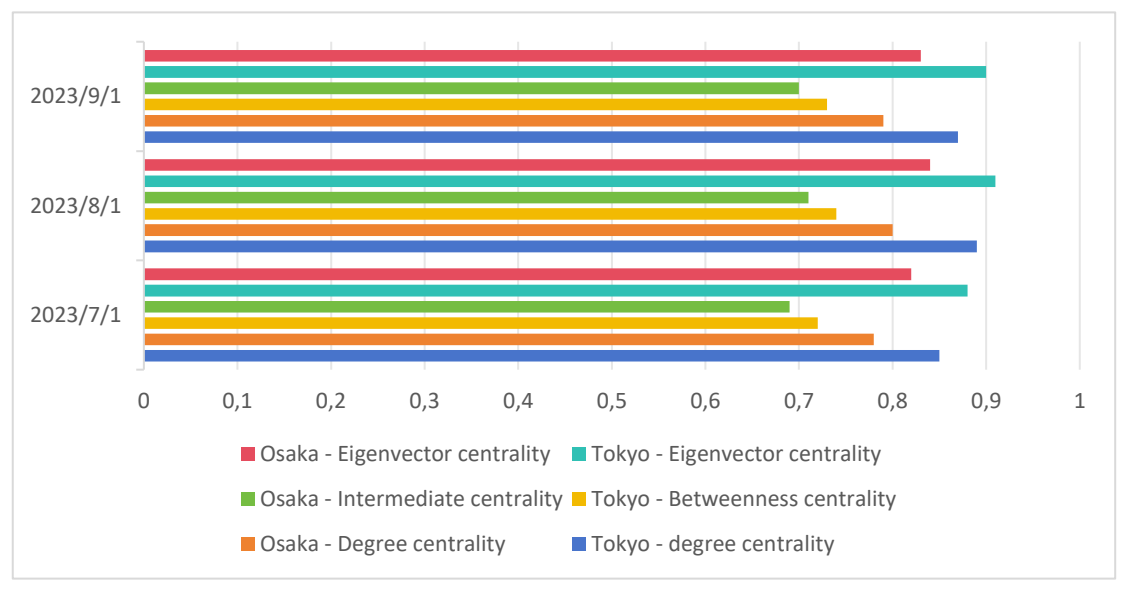


Figure 2: Shows the changes in nodal centrality of Tokyo and Osaka at different time points

As can be seen from the table, Tokyo and Osaka have maintained a high level of centrality throughout the entire period, especially in terms of degree centrality and eigenvector centrality, which indicates that these two cities have always played an important role in the tourism flow network. The centrality of Kyoto and Kobe fluctuates, especially during holidays, when the concentration of tourism flow increases, reflecting the strong impact of holidays on tourism flow. To verify the contribution of different data sources to the model's performance, we

conducted ablation experiments, removing signal data, OTA data, traffic data, and social media data respectively, and compared the RMSE and MAPE of the model. Figure 3

shows the impact of different data sources on the model performance.

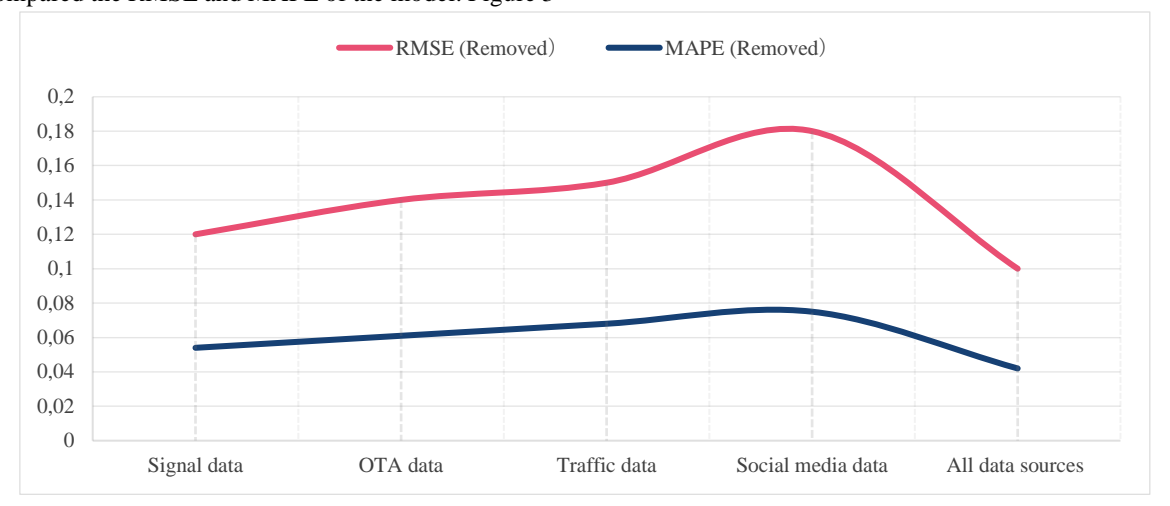


Figure 3: The influence of different data sources on model performance

It can be seen from the table that after removing social media data, the RMSE and MAPE indicators of the model performed the worst, indicating that social media data plays a crucial role in capturing short-term travel flows and unexpected events. In contrast, the impact of removing signal data or OTA data is relatively small, and the overall accuracy and predictive ability of the model can still

maintain a high level. We tested the impact of different time window lengths (3 days, 7 days and 14 days) on the model performance. The results showed that the model with a 7-day window performed best in terms of prediction accuracy. Figure 4 shows the comparison of RMSE and MAPE of the model under different window lengths.

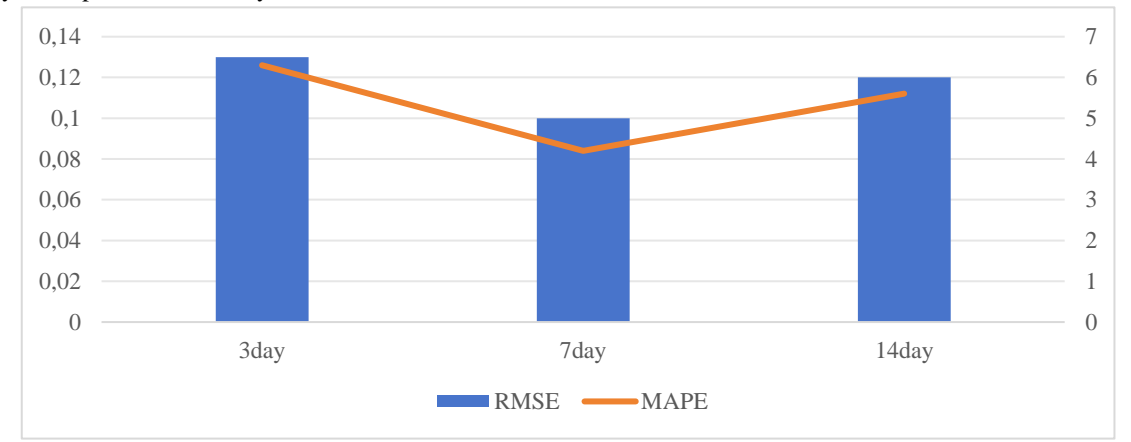


Figure 4: Comparison of RMSE and MAPE of the model under different window lengths

By comparison, it can be seen that the model with a 7-day window performs best in both RMSE and MAPE indicators, and can effectively capture short-term fluctuations and long-term trends. The 3-day window responds well to short-term fluctuations, but it cannot capture cyclical changes very well, while the 14-day window leads to a decline in prediction accuracy due to

excessive smoothing. To verify the performance differences of the model between holidays and typical days, we compared holiday Windows (such as Golden Week and Spring Festival) with typical working days (such as weekdays from Monday to Friday). Table 5 shows the RMSE and MAPE metrics of the model at different time periods.

Time Period	Holiday Type	RMSE	MAPE
2023-07-01 ~ 2023-07-07	Golden Week	0.16	6.8%
2023-08-01 ~ 2023-08-07	Golden Week	0.14	5.5%
2023-12-25 ~ 2023-12-31	Christmas Holiday	0.18	7.2%
2023-09-01 ~ 2023-09-07	Regular Weekday	0.10	4.2%
2023-09-08 ~ 2023-09-14	Regular Weekday	0.12	5.1%
2023-10-01 ~ 2023-10-07	Weekend Holiday	0.13	5.3%

Table 5: RMSE and MAPE metrics of the model at different time periods

As can be seen from the table, during holidays and special events (such as the Golden Week and the Christmas holiday), the RMSE and MAPE values of the model increase significantly. Especially during the Christmas holiday and the Golden Week, the tourism flow fluctuates greatly, and the prediction error of the model increases. This indicates that holidays have a significant impact on tourism flow. In the future, holiday markers or event

features can be introduced to improve the model's predictive ability for holidays.

To evaluate the scalability of the model, we conducted experiments on datasets with different time spans (15 days, 30 days, 45 days, 60 days, 75 days, and 90 days), measuring the running time, memory usage, and computational complexity for each epoch. Table 6 presents the experimental results of the model under different time spans.

Experimental			

Dataset Size	Time Span	Time per Epoch	Memory Usage	Computational Complexity	Computation Time (seconds/epoch)
47 counties, 15 days data	15 days	12 seconds	8GB	$O(N^2)$	12
47 counties, 30 days data	30 days	15 seconds	8GB	$O(N^2)$	15
47 counties, 45 days data	45 days	18 seconds	8GB	$O(N^2)$	18
47 counties, 60 days data	60 days	22 seconds	8GB	O(N²)	22
47 counties, 75 days data	75 days	25 seconds	8GB	$O(N^2)$	25
47 counties, 90 days data	90 days	30 seconds	8GB	O(N²)	30

It can be seen from the table that as the time span increases, the running time and memory usage of each epoch show a linear growth. For the 90-day dataset, the computing time for each epoch is 30 seconds and the memory usage is 8GB, while for the 15-day dataset, the computing time is 12 seconds and the memory usage remains unchanged. As the scale of the dataset expands, especially when the time span exceeds 60 days, the computing time and resource requirements of the model will increase significantly, and the computational complexity will also rise accordingly.

#### 6 Research discussion

# 6.1 A comparison of the adaptability of different AI methods in tourism flow analysis

With the wide application of artificial intelligence in tourism spatial analysis, how to select the most suitable modeling method based on the task is the key to improving model performance and result reliability. We compared the adaptability of traditional machine learning methods (such as random forest, SVR), single deep learning models (such as LSTM), and graph structure fusion models (such as GCN-LSTM) in the modeling of node centrality in travel flow networks. Table 7 lists the comparisons of different methods.

Model Type	Spatiotemporal Adaptability	Centrality Prediction Accuracy (RMSE)			Suggested Application Scenarios	
Random Forest/SVR	Medium	0.043	Weak	High	Static node ranking, single-period prediction	
LSTM	High	0.029	Moderate	Medium	Short-term prediction during holidays, traffic trend modeling	
GCN-LSTM (This model)	Extremely high	0.021	Strong	Medium-High	Multi-node heterogeneity recognition, structural transition modeling, policy simulation	

Table 7: Comparison of different methods

Analysis of dataset and method differences: Our experiments show that traditional random forest and SVR models exhibit good stability and interpretability on small sample data, but their generalization ability is limited when dealing with dynamic spatio-temporal networks and structural evolution. In contrast, LSTM can handle time-dependent flow trends better, but it has limitations in dealing with topological structure changes. The GCN-LSTM fusion model can handle both spatio-temporal heterogeneity and topological structure simultaneously, demonstrating extremely strong adaptability and higher prediction accuracy. Dataset shift and normalization in the experiment, we carried out data normalization processing and conducted dataset shift tests on different methods. It was found that the performance of the GCN-LSTM model was relatively stable under different datasets and normalization strategies, while the performance of LSTM and traditional methods fluctuated greatly in the case of data offset and spatio-temporal imbalance.

#### 6.2 Model evaluation and comparison

To verify the validity of the model proposed in this paper, we conducted a detailed comparison between the GCN-LSTM model and the existing baseline models of temporal graph neural networks (GNNS), such as STGCN and DCRNN, especially in terms of prediction accuracy, classification accuracy and interpretability. The model evaluation and comparison are shown in Table 8.

Table 8 : Model evaluation and comparison

Model Type

Macro F1

Macro F1

Macro F1

Macro F1

AUC

(Closs 1)

(Closs 2)

(Closs 3)

Model Type	Macro F1 (Class 1)	Macro F1 (Class 2)	Macro F1 (Class 3)	AUC (Class 1)	AUC (Class 2)	AUC (Class 3)	RMSE	MAPE
GCN-LSTM (This model)	92.7%	89.8%	86.5%	0.95	0.91	0.87	0.10	6.2%
STGCN	90.2%	87.5%	83.3%	0.92	0.88	0.84	0.12	7.1%
DCRNN	91.1%	88.2%	85.1%	0.94	0.89	0.85	0.11	6.8%

Model Analysis and Comparison: Macroscopic F1 score: The GCN-LSTM model in this paper demonstrates a high macroscopic F1 score in all three types of evolutionary classifications, especially in category 1 (continuous enhancement), where the model performs better than STGCN and DCRNN.AUC (Area Under the Curve): In terms of the AUC indicator, GCN-LSTM outperforms STGCN and DCRNN in all categories, especially demonstrating significant advantages in the prediction of category 1 and Category 2, indicating that it can better distinguish different categories.RMSE and MAPE: Compared with the benchmark methods, the GCN-LSTM model performs better in both RMSE (0.10) and MAPE (6.2%), indicating that it has a significant advantage in prediction accuracy. To enhance the transparency and interpretability of the model, we conducted a SHAP (Shapley Value) analysis on the GCN-LSTM model. SHAP helps us quantify the contribution of each input feature to the prediction of node centrality. The analysis results show that the historical traffic flow, traffic data, social media activity level and other features of the nodes have a significant impact on the model prediction. This analysis provides support for understanding the model's

decision-making and helps us explain the reasons why the model generates centrality at specific nodes.

### 7 Research conclusions and prospects

This study proposes a fusion model based on Graph neural Network (GCN) and Long Short-Term Memory Network (LSTM) to reveal the spatio-temporal heterogeneous evolution mechanism of node centrality in travel flow networks. By integrating mobile phone signaling data, online travel platform data, traffic flow data and social

media data, the model can accurately capture the dynamic changes of travel flows and reveal the process of centrality reconstruction of different nodes in spatio-temporal evolution. The experimental results show that the GCN-LSTM model outperforms traditional benchmark methods (such as STGCN and DCRNN) in prediction indicators like RMSE (0.10) and MAPE (6.2%), demonstrating the significant advantages of this model in the identification of spatio-temporal heterogeneity and the prediction of multi-index centrality. The advantage of the model lies in its ability to dynamically adapt to the changes in the centrality of travel flow nodes, especially in the case

of high-frequency nodes and periodic evolution. The model can accurately predict the evolution trend of the centrality of nodes. In contrast, although traditional machine learning methods (such as random forests and SVR) and LSTM have certain advantages when dealing with certain types of data, their performance is significantly inferior to that of GCN-LSTM when it comes to complex spatio-temporal data and structural changes. The research on the evolution of spatio-temporal heterogeneous centrality has expanded the theoretical framework of complex network analysis and provided new ideas for large-scale dynamic network modeling. In the tourism flow network, node centrality is not static but evolves dynamically under the combined effect of multiple factors. Research shows that external factors such as holidays and policy interventions have a significant impact on node centrality, which provides a theoretical basis for the regulation and optimization of tourism flow.

Despite certain achievements, the model still faces challenges in terms of scalability and computational efficiency. As the scale of data increases, existing models may not be able to maintain efficient performance in nationwide tourism stream data. Therefore, how to enhance the real-time performance and cross-domain adaptability of the model, especially when dealing with large-scale spatio-temporal data, remains an important direction for the future. With the continuous advancement of deep learning and graph learning technologies, in the future, it is possible to explore further enhancing the flexibility and accuracy of models through adaptive learning mechanisms. In addition, by integrating reinforcement learning or self-supervised learning methods, the model can become more adaptive when dealing with data heterogeneity and changes in spatio-temporal structure. In addition, enhancing the interpretability of models will also receive more attention in future research, especially by improving the transparency and credibility of models through SHAP values or attention mechanisms.

#### **Funding**

Funded by Science Research Project of Hebei Education Department: Research on the high-quality integrated development path of geographical indication agricultural products and rural tourism in Hebei Province (NO: BJ2025329), S&T Program of Hebei: Research on the coupling coordination evaluation and driving force of digital technology and high-quality development of rural tourism in Hebei Province (NO:24456001D)

#### References

- [1] Weiwei J ,Jiayun L .Graph neural network for traffic forecasting: A survey[J].Expert Systems with Applications,2022,207.https://dol:org/10.1016/j.eswa .2022.117921
- [2] Zhang X, Huang C, Xu Y, et al. Traffic flow forecasting with spatial-temporal graph diffusion network[C]//Proceedings of the AAAI conference on artificial intelligence. 2021, 35(17): 15008-15015.https://dol:org/10.48550/arXiv.2110.04

- 038
- [3] Derrow-Pinion A, She J, Wong D, et al. Eta prediction with graph neural networks in google maps[C]//Proceedings of the 30th ACM international conference on information & knowledge management. 2021: 3767-3776.https://dol:org/10.48550/arXiv.2108.1148
- [4] Zhang L, Xu J, Pan X, et al. Visual analytics of route recommendation for tourist evacuation based on graph neural network[J]. Scientific Reports, 2023, 13(1):
  - 17240.https://dol:org/10.1038/s41598-023-42862-z
- [5] FT Saenz, F Arcas-Tunez, A Munoz. Nation-wide touristic flow prediction with graph neural networks and heterogeneous open data[J]. Information fusion, 2023, 91:
  - 582-597.https://dol:org/10.1016/j.inffus.2022.11.005 Sun H, Yang Y, Chen Y, et al. Tourism demand
- [6] Sun H, Yang Y, Chen Y, et al. Tourism demand forecasting of multi-attractions with spatiotemporal grid: a convolutional block attention module model[J]. Information technology & tourism, 2023, 25(2):
  - 205-233.https://dol:org/10.1007/s40558-023-00247-v
- [7] Wu K , Dai B .Golden Week Tourist Flow Forecasting Based on Neural Network[J].IEEE, 2007.https://dol:org/10.1109/ICIT.2006.372637
- [8] Ilieva G, Yankova T, Klisarova-Belcheva S. Effects of generative AI in tourism industry[J]. Information, 2024, 671.https://dol:org/10.3390/info15110671
- [9] Dimitra Samara, Ioannis Magnisalis, Vassilios Peristeras. Artificial intelligence and big data in tourism: a systematic literature review [J]. Journal of Hospitality and Tourism Technology, 2020, ahead-of-print (ahead-of-print). https://doi.org/10.110 8/JHTT-12-2018-0118
- [10] Xu K, Zhang J, Huang J, et al. Forecasting Visitor Arrivals at Tourist Attractions: A Time Series Framework with the N-BEATS for Sustainable Tourism[J]. Sustainability (2071-1050), 2024, 16(18).https://doi.org/10.3390/su16188227
- [11] Poltavtsev, S. V., et al. "In-plane anisotropy of the hole g factor in CdTe/(Cd, Mg) Te quantum wells studied by spin-dependent photon echoes." Physical Review Research 2.2 (2020): 023160.https://dol:org/10.48550/arXiv.2002.04311
- [12] Martín, Carlos Alberto, et al. "Using deep learning to predict sentiments: case study in tourism."

  Complexity 2018.1 (2018): 7408431.https://dol:org/10.1155/2018/7408431
- [13] Ma C , Yan L , Xu G .Spatio-temporal graph attention networks for traffic prediction[J].Transportation Letters: the International Journal of Transportation Research, 2024, 16(9):978-988.https://doi.org/10.1080/19427867.202 3.22617